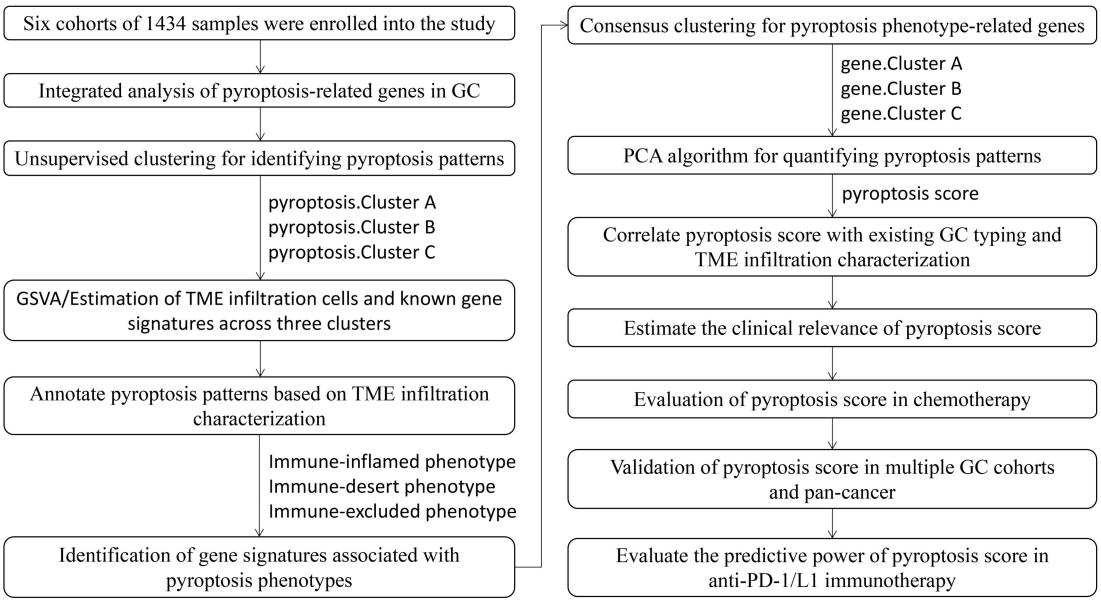

Figure S1. Summary of this study.

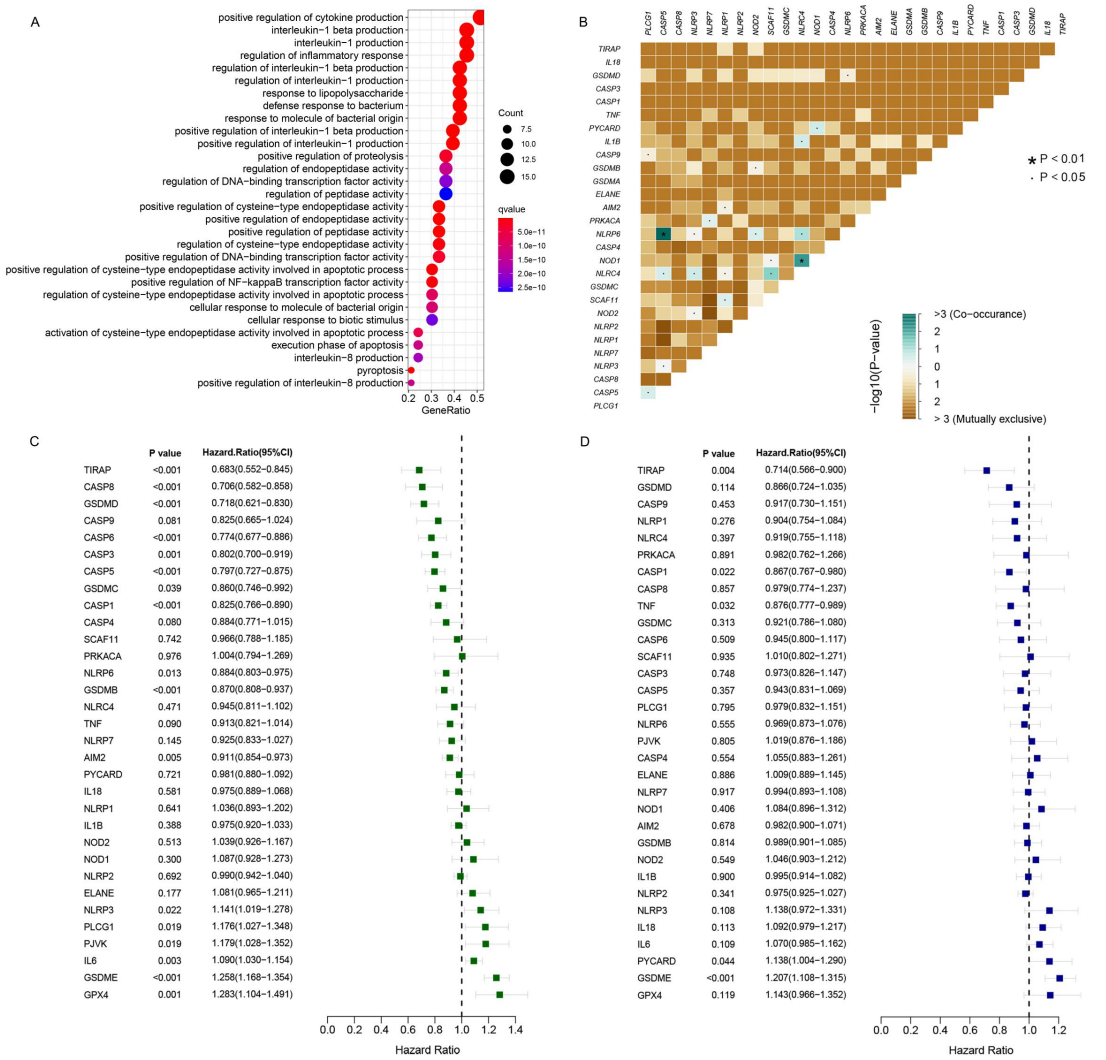

Figure S2. Comprehensive analysis of 33 PRs based on the TCGA cohort. (A) The KEGG enrichment analysis of PRs. The x-axis represented gene ratio. **(B)** The mutation co-occurrence and exclusion analyses for PRs. Co-occurrence, green; Exclusion, brown. **(C)** Univariate analysis for PRs. **(D)** Multivariate analysis for PRs.

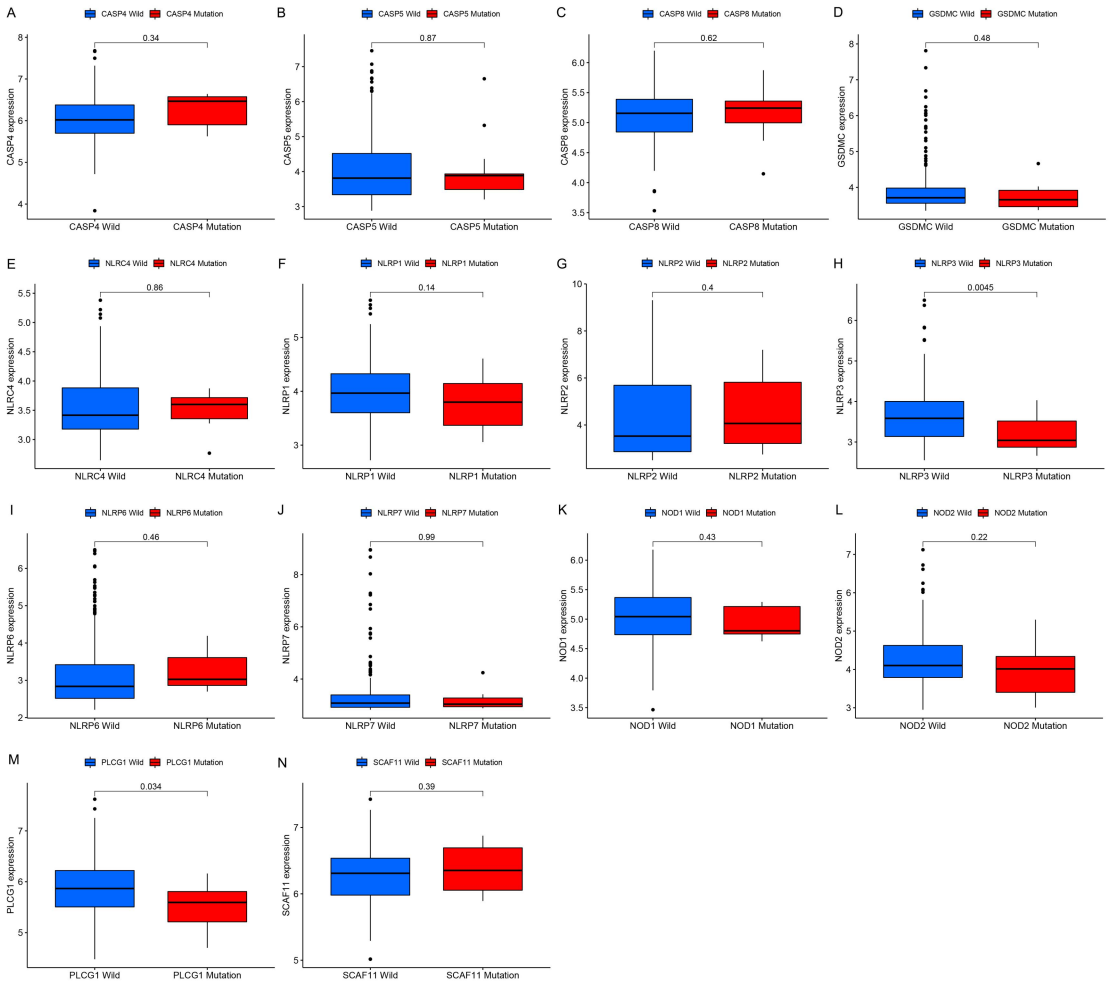

Figure S3. Correlation between PRs mutation and their expression. (A) *CASP4*. **(B)** *CASP5*. **(C)** *CASP8*. **(D)** *GSDMC*. **(E)** *NLRC*4. **(F)** *NLRP1*. **(G)** *NLRP2*. **(H)** *NLRP3*. **(I)** *NLRP*6. **(J)** *NLRP7*. **(K)** *NOD1*. **(L)** *NOD2*. **(M)** *PLCG1*. **(N)** *SCAF11*.

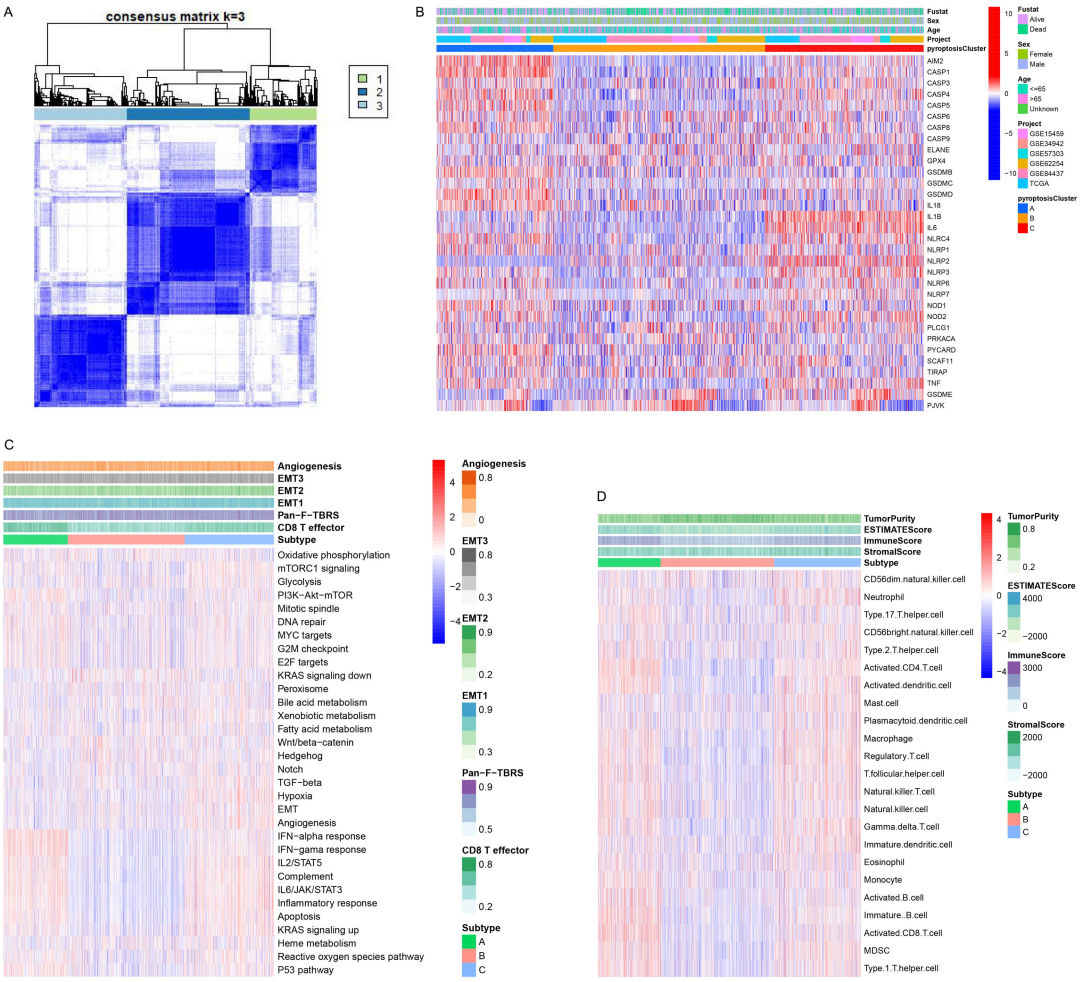

Figure S4. Unsupervised clustering of PRs in the meta-cohort, and transcriptome traits and TME characteristics in distinct pyroptosis patterns. (A) Consensus matrice for k = 3. **(B)** The heatmap of the expression of PRs in distinct pyroptosis patterns. Six GC cohorts were used as sample annotations. **(C)** The heatmap of enrichment levels of well-defined biological signatures in three pyroptosis patterns. **(D)** The heatmap of the fraction of TME infiltrating cells in distinct pyroptosis patterns.

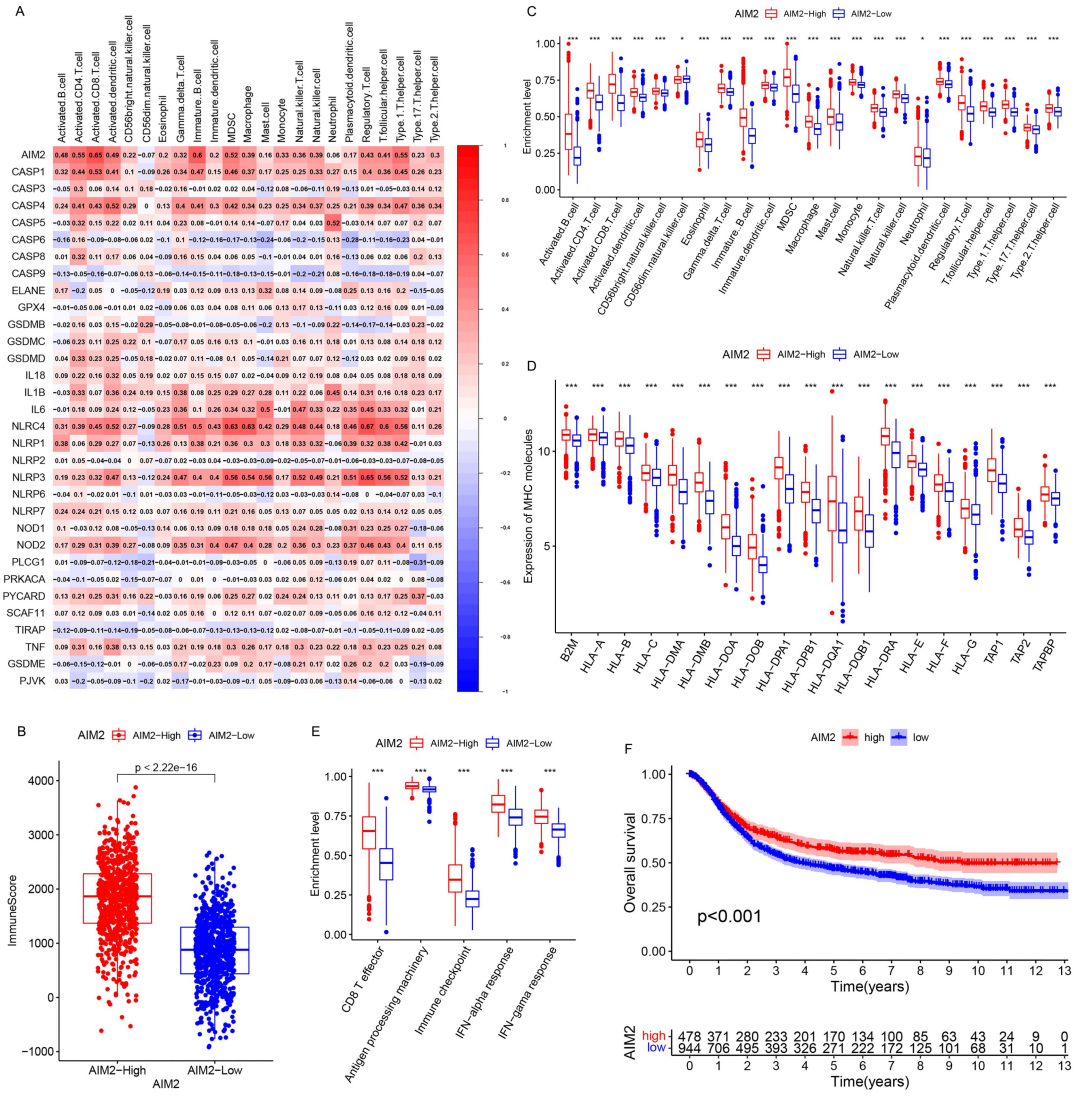

Figure S5. Correlation between TME infiltration cells and PRs and the role of *AIM2* in GC. (A) The correlation between each TME infiltration cell type and each PR using spearman analysis. Negative correlation was marked with blue and positive correlation with red. **(B)** Difference in immune score between *AIM2* high expression and low expression. ($P < 0.00001$, Wilcoxon test). **(C)** Difference in the abundance of each TME infiltrating cell between *AIM2* high expression and low expression groups. The upper and lower ends of the boxes represented interquartile range of values. The lines in the boxes represented median value. (*$P < 0.05$; **$P < 0.01$; ***$P < 0.001$). **(D)** Difference in the expression of MHC molecules between *AIM2* high expression and low expression groups. (*$P < 0.05$; **$P < 0.01$; ***$P <$ 0.001). **(E)** Differences in immune-activated pathways between *AIM2* high expression and low expression groups. (*$P < 0.05$; **$P < 0.01$; ***$P < 0.001$). **(F)** Kaplan-Meier analysis for patients with low or high *AIM2* expression in the meta-cohort (Log-rank test: $P < 0.001$).

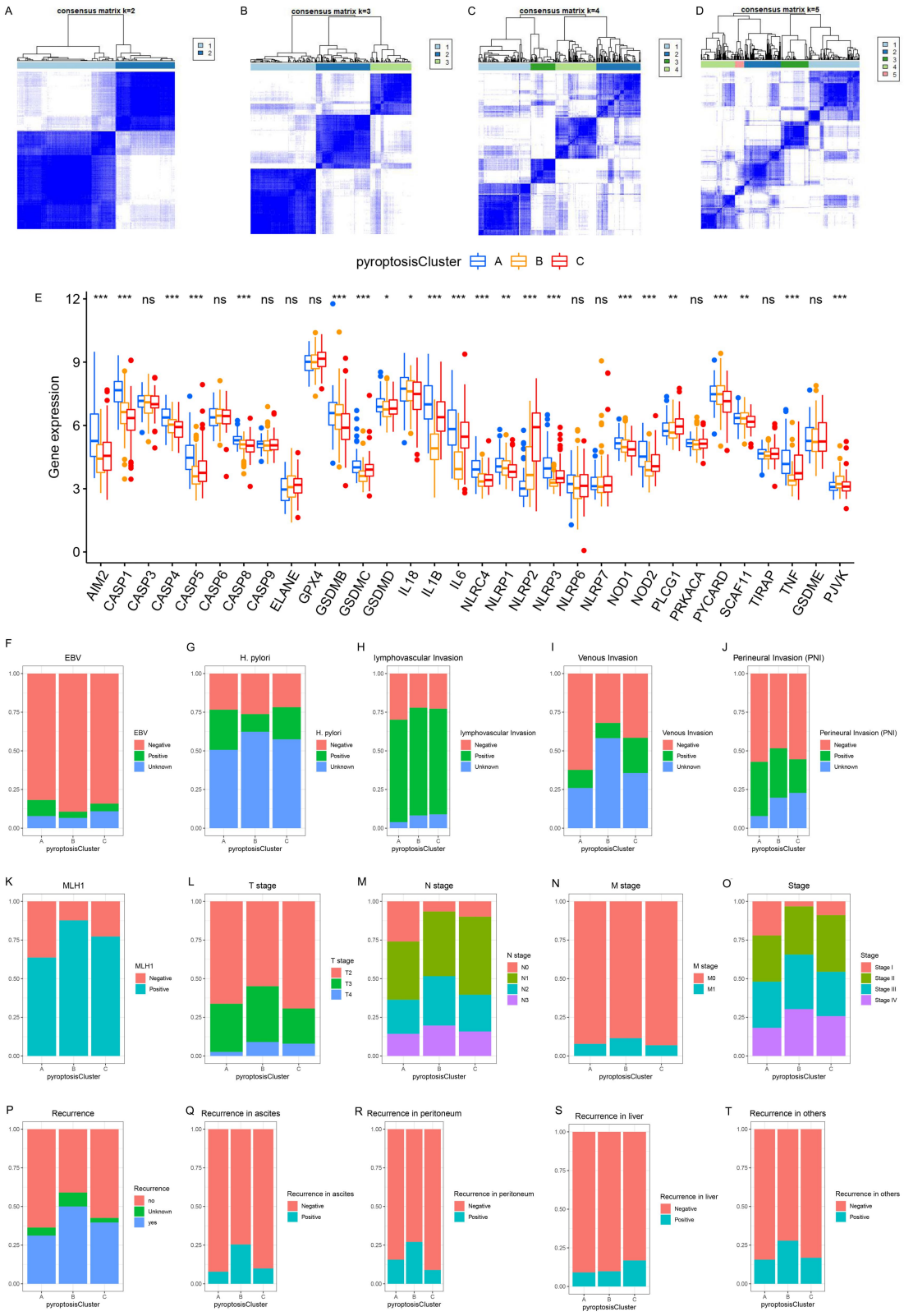

Figure S6. Unsupervised clustering of PRs in GSE62254/ACRG cohort and clinicopathologic traits in three pyroptosis patterns. (A-D) Consensus matrices for k = 2-5. **(E)** Differential expression analysis of PRs in distinct pyroptosis patterns. **P* < 0.05; ***P* < 0.01; ****P* < 0.001. **(F-T)** The proportion of clinicopathologic traits in three pyroptosis patterns. **(F)** EBV. **(G)** H. pylori. **(H)** Lymphovascular invasion. **(I)** Venous invasion. **(J)**

Perineural invasion. **(K)** MLH1. **(L)** T stage. **(M)** N stahe. **(N)** M stage. **(O)** Stage. **(P)** Recurrence. **(Q)** Recurrence in ascites. **(R)** Recurrence in peritoneum. **(S)** Recurrence in liver. **(T)** Recurrence in others.

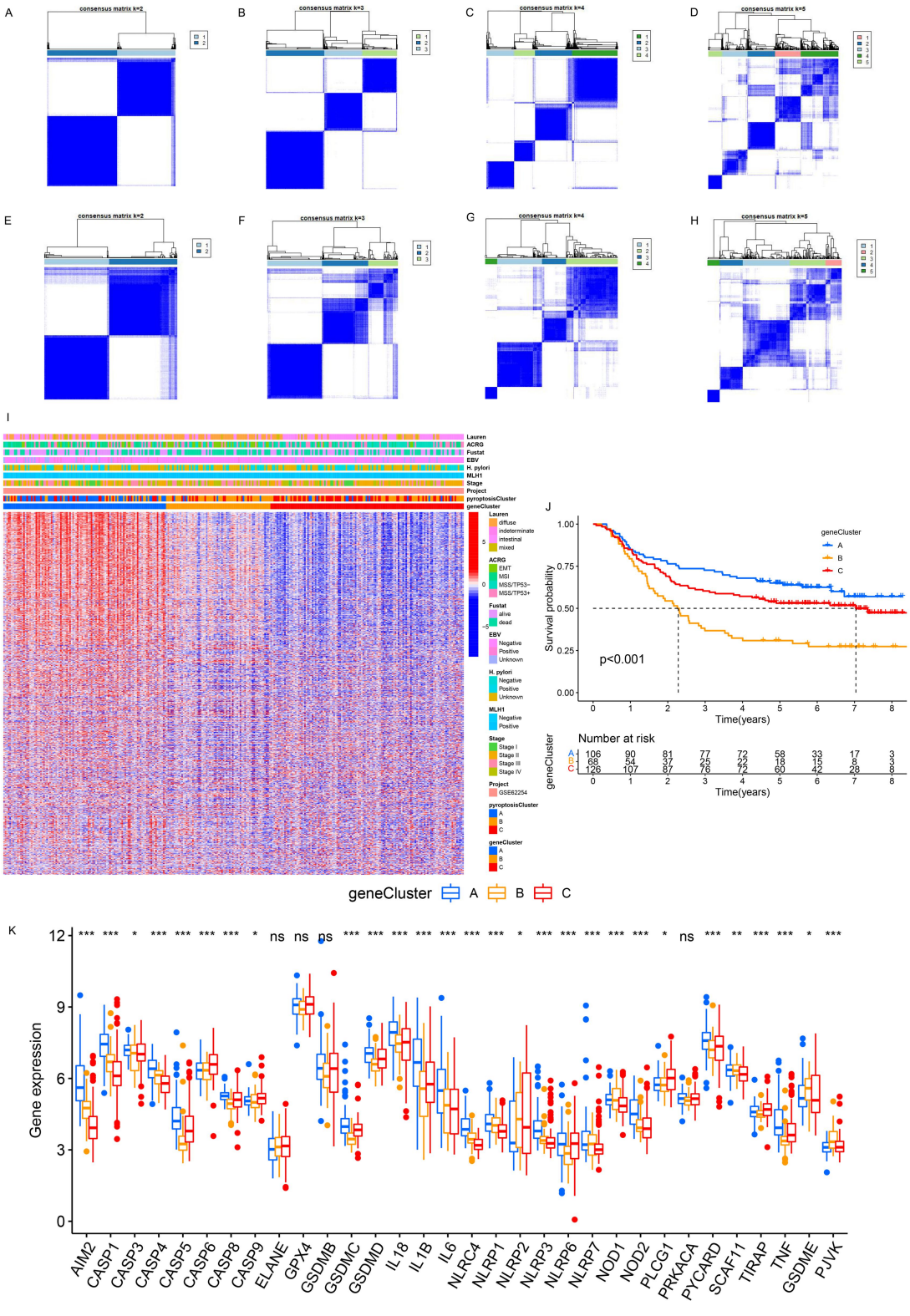

Figure S7. Unsupervised clustering of pyroptosis pattern-related genes in

GSE62254/ACRG cohort. (A-D) Consensus matrices for k = 2 - 5 in the meta-cohort. **(E-H)** Consensus matrices for k = 2 - 5 in GSE62254/ACRG cohort. **(I)** Unsupervised clustering of overlapping pyroptosis pattern-related genes in GSE62254/ACRG cohort divided patients into three genomic subtypes, called gene cluster A-C, respectively. The lauren subtypes, ACRG subtypes, suvival status, EBV infection, H. pylori infection, MLH1, tumor stage, datasets, pyroptosis patterns and gene clusters were used as patient annotations. **(J)** Kaplan-Meier analysis for three distinct gene clusters with 300 GC patients in GSE52254/ACRG cohort (Log-rank test: $P < 0.001$). **(K)** The expression of PRs in three gene clusters the GSE62254/ACRG cohort. The upper and lower ends of the boxes represented an interquartile range of values. The lines in the boxes represented the median value. (one-way ANOVA test: $*P < 0.05$; $**P < 0.01$; $***P < 0.001$).

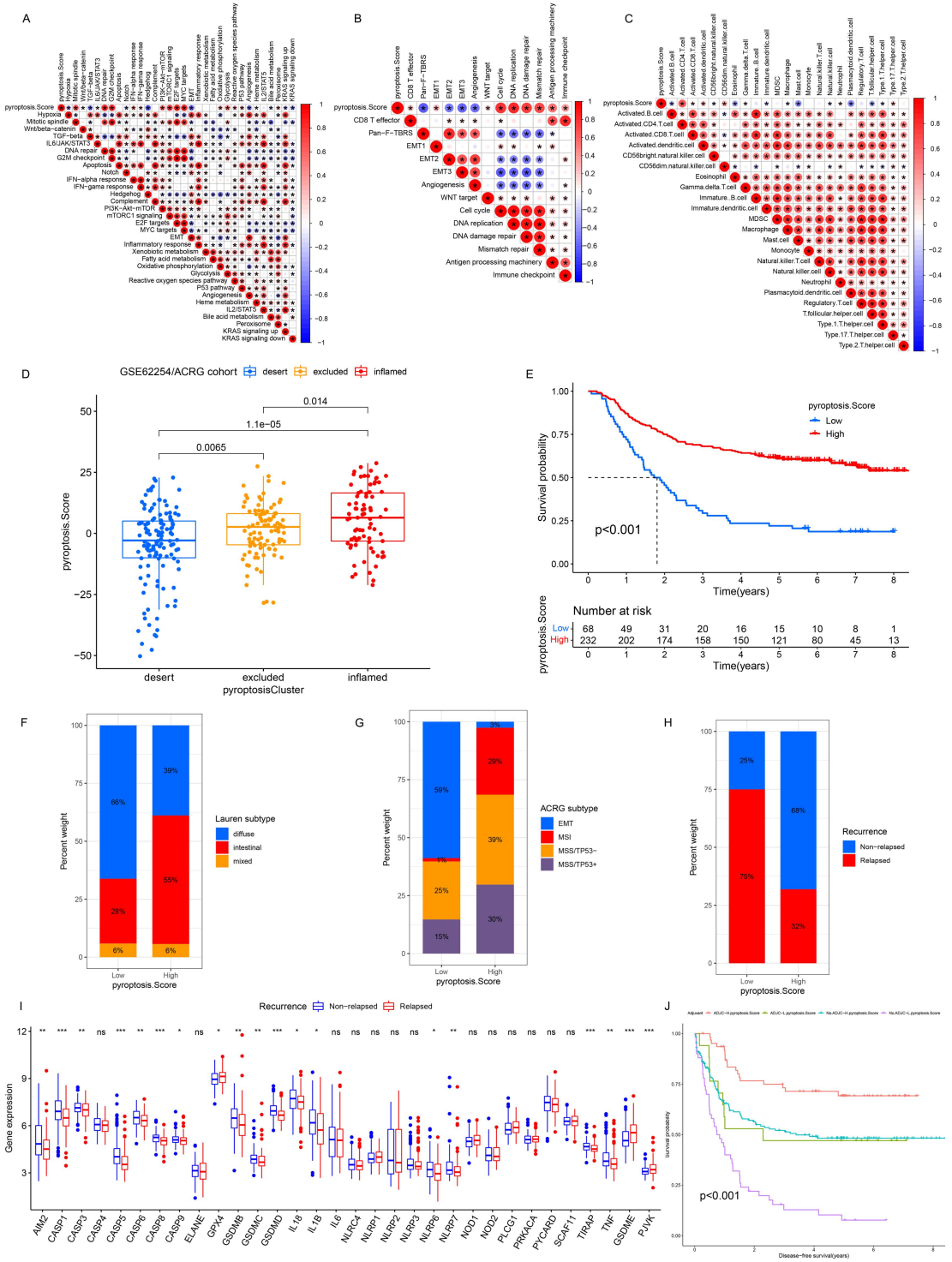

Figure S8. Correlation between PS and TME status and relevant biological signatures in GSE62254/ACRG cohort. (A-C) The correlation between PS and Hallmark pathways **(A)**, Mariathasan et al. constructed gene sets **(B)**, and TME infiltration cells **(C)** using spearman analysis. Negative correlation was marked with blue and positive correlation with red. $P < 0.05$. **(D)** Differences in PS among three TME phenotypes in GSE62254/ACRG cohort ($P < 0.05$, Kruskal-Wallis test). **(E)** Kaplan-Meier analysis for patients in high and low PS subgroups in GSE62254/ACRG cohort (Log-rank test: $P < 0.001$). **(F)** The fraction of patients with Lauren subtypes in low- or high-PS subgroups. **(G)** The fraction of patients with ACRG

subtypes in low- or high-PS subgroups. **(H)** The fraction of patients with (or without) recurrence in low- or high-PS subgroups. **(I)** Difference in the expression of PRs between relapsed and non-relapsed subgroups. The upper and lower ends of the boxes represented interquartile range of values. The lines in the boxes represented median value. (*$P < 0.05$; **$P < 0.01$; ***$P < 0.001$). **(J)** Disease-free survival analyses for subgroup patients stratified by both PS and treatment with adjuvant chemotherapy using Kaplan-Meier curves. H, high; L, Low; ADJC, adjuvant chemotherap (Log-rank test: $P < 0.001$).

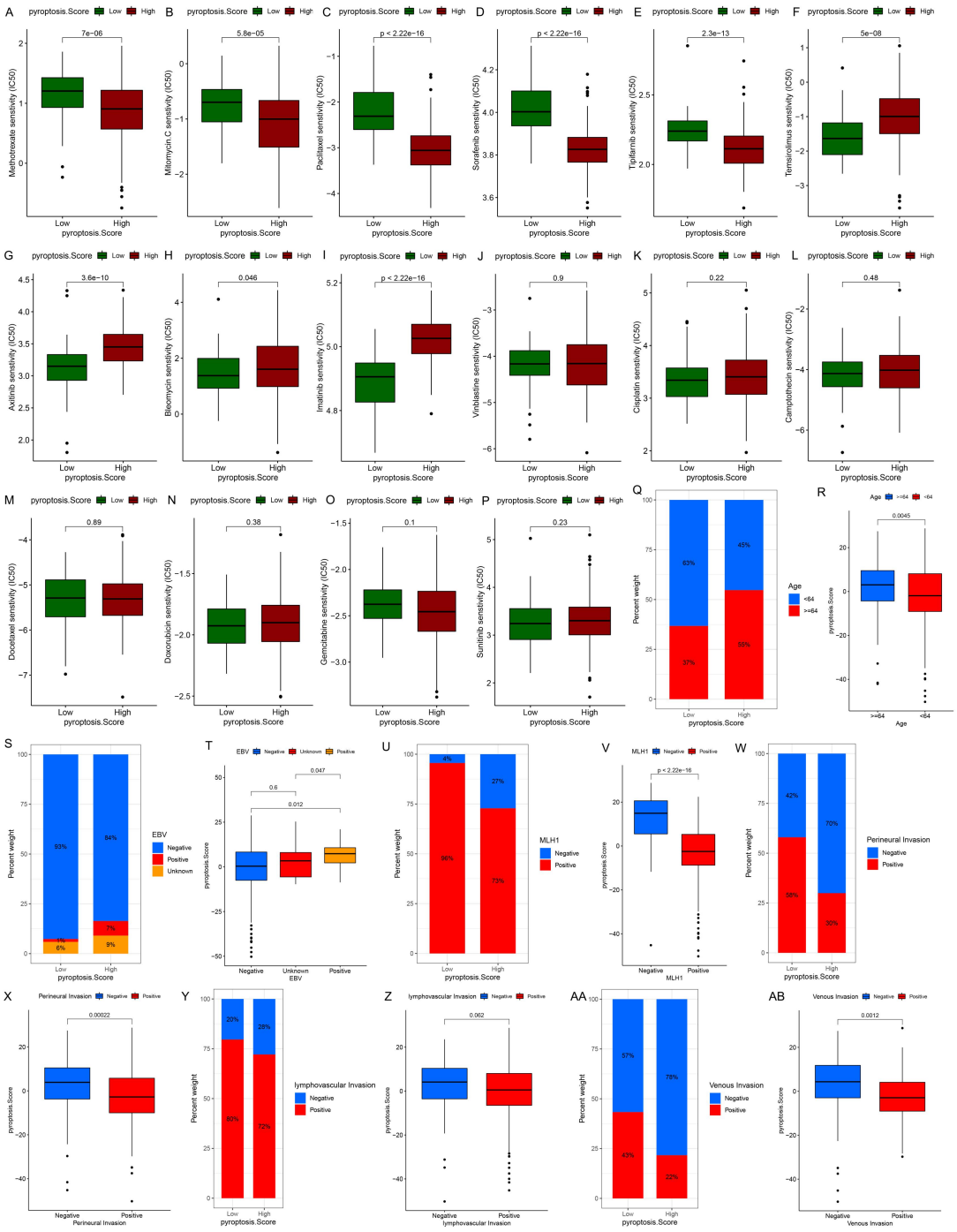

Figure S9. Prediction of therapeutic sensitivity for multiple compounds in GSE62254/ACRG cohort. **(A)** Methotrexate. **(B)** Mitomycin C. **(C)** Paclitaxel. **(D)** Sorafenib. **(E)** Tipifarnib. **(F)** Temsirolimus. **(G)** Axitinib. **(H)** Blemycin. **(I)** Imatinib. **(J)** Vinblastine. **(K)** Cisplatin. **(L)** Camptothecin. **(M)** Docetaxel. **(N)** Doxorubicin. **(O)** Gemcitabine. **(P)** Sunitinib. **(Q-AB)** Difference in PS among distinct clinical subgroups in GSE62254/ACRG cohort. **(Q, R)** Age. **(S, T)** EBV infection status. **(U, V)** MLH1. **(W, X)** perineural invasion. **(Y, Z)** lymphovascular invasion. **(AA, AB)** venous invasion.

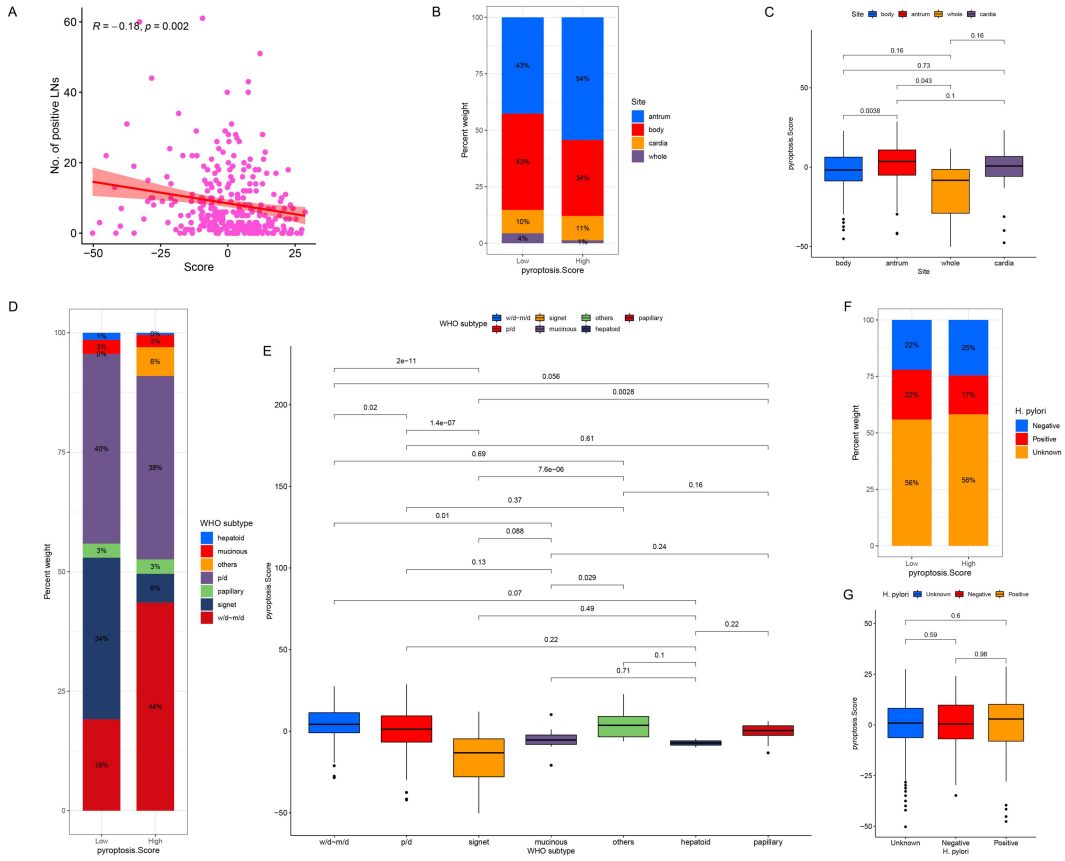

Figure S10. Correlation between PS and clinicopathologic traits in GSE62254/ACRG cohort. **(A)** Correlation analysis between PS and the number of positive lymph nodes. **(B)** The fraction of patients with different tumor sites in low- or high-PS subgroups. **(C)** Differences in PS among different tumor sites. **(D)** The fraction of patients with WHO subtypes in low- or high-PS subgroups. **(E)** Differences in PS among distinct WHO subtypes. **(F)** The fraction of patients with different H.pylori infection status in low- or high-PS subgroups. **(G)** Differences in PS among patients with different H.pylori infection status.

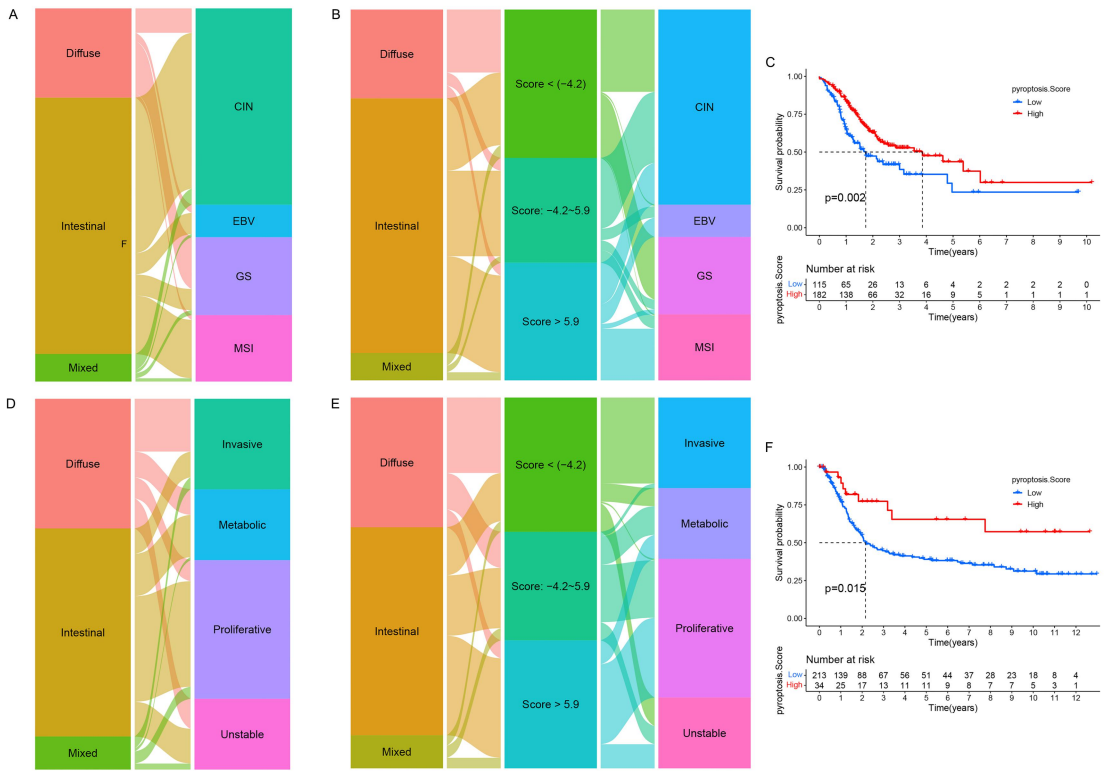

Figure S11. Correlation between PS and TCGA typing and Lei typing. (A) Alluvial diagram of Lauren subtypes (diffuse, intestinal and mix) in groups with different TCGA subtypes (CIN, EBV, GS and MSI) in the TCGA cohort. **(B)** Alluvial diagram of PS in groups with different Lauren subtypes and TCGA subtypes in the TCGA cohort. **(C)** Survival analysis of PS in the TCGA cohort. **(D)** Alluvial diagram of Lauren subtypes (diffuse, intestinal and mix) in groups with different Lei subtypes (invasive, metabolic, proliferative and unstable) in Lei cohort (GSE15459 and GSE34942). **(E)** Alluvial diagram of PS in groups with different Lauren subtypes and Lei subtypes in Lei cohort (GSE15459 and GSE34942). **(F)** Survival analysis of PS in Lei cohort (GSE34942 and GSE15459).

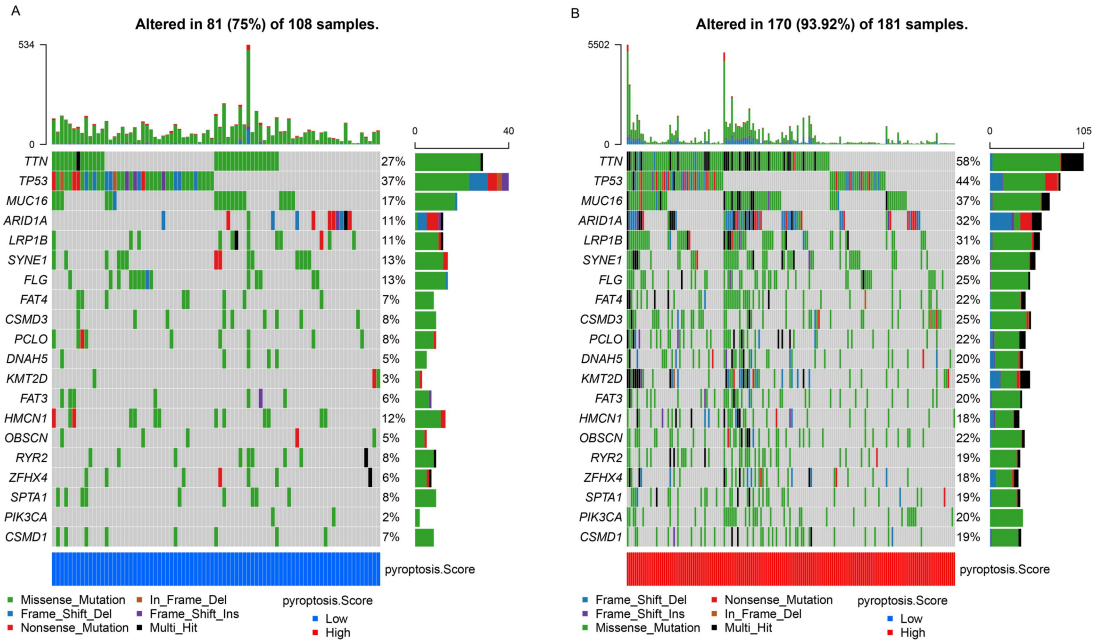

Figure S12. Correlation between PS and tumor somatic mutation. (A-B) Landscapes of tumor somatic mutation stratified by high- **(A)** and low-PS **(B)** subgroups in the TCGA cohort. Each column represented individual patients. The upper barplot showed TMB. The number on the right indicated the mutation frequency in each gene. The right barplot showed the proportion of each variant type.

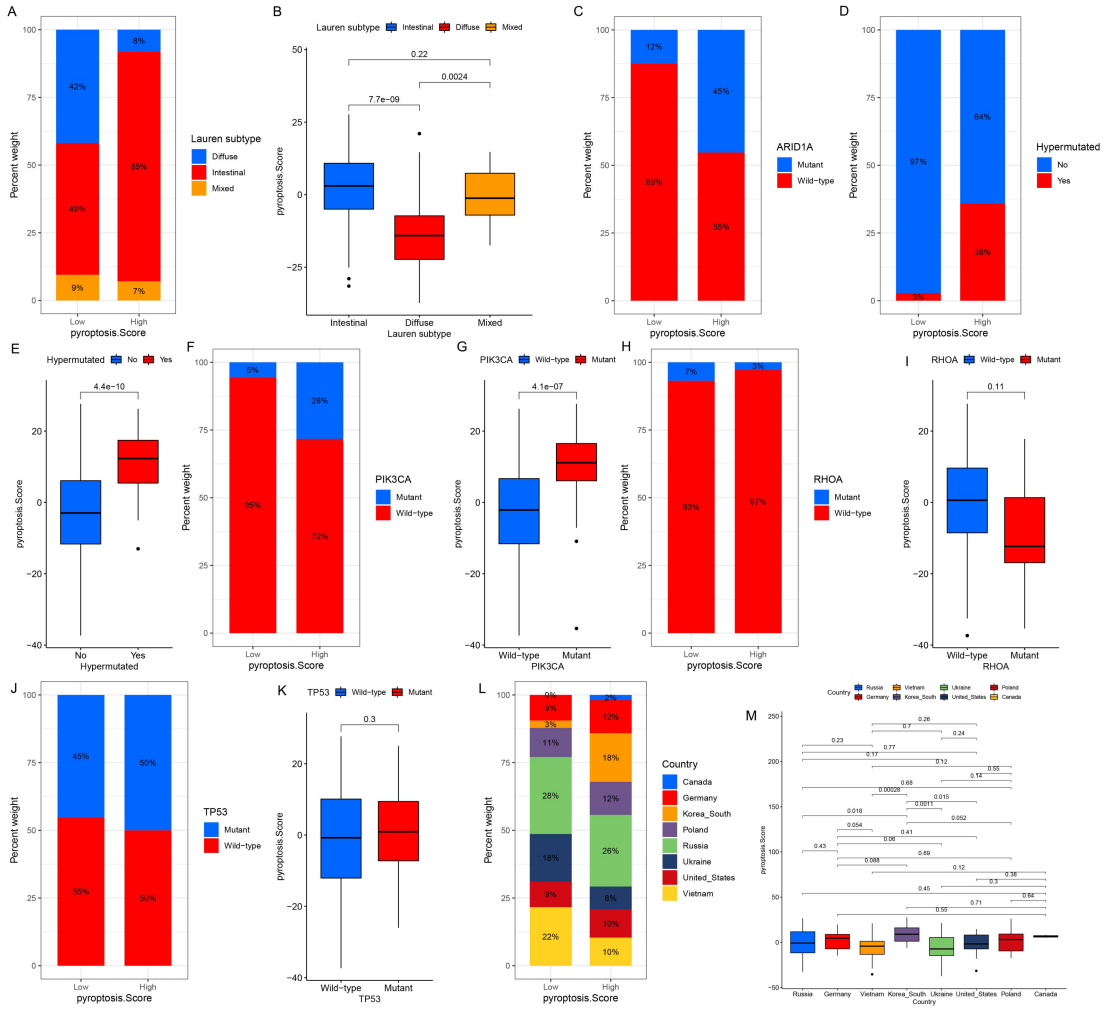

Figure S13. Correlation between PS and clinicopathologic traits in the TCGA cohort. (A) The fraction of patients with Lauren subtypes in low- or high-PS subgroups. **(B)** Differences in PS among different Lauren subtypes. **(C)** The fraction of patients with mutant type and wild type of *ARID1A* in low- or high-PS subgroups. **(D)** The fraction of patients with hypermutated type and hypomutated type in low- or high-PS subgroups. **(E)** Differences in PS among hypermutated type and hypomutated type. **(F)** The fraction of patients with mutant type and wild type of *PIK3CA* in low- or high-PS subgroups. **(G)** Differences in PS among mutant type and wild type of *PIK3CA*. **(H)** The fraction of patients with mutant type and wild type of *RHOA* in low- or high-PS subgroups. **(I)** Differences in PS among mutant type and wild type of *RHOA*. **(J)** The fraction of patients with mutant type and wild type of *TP53* in low- or high-PS subgroups. **(K)** Differences in PS among mutant type and wild type of *TP53*. **(L)** The fraction of patients from different countries in low- or high-PS subgroups. **(M)** Differences in PS among patients from different countries.

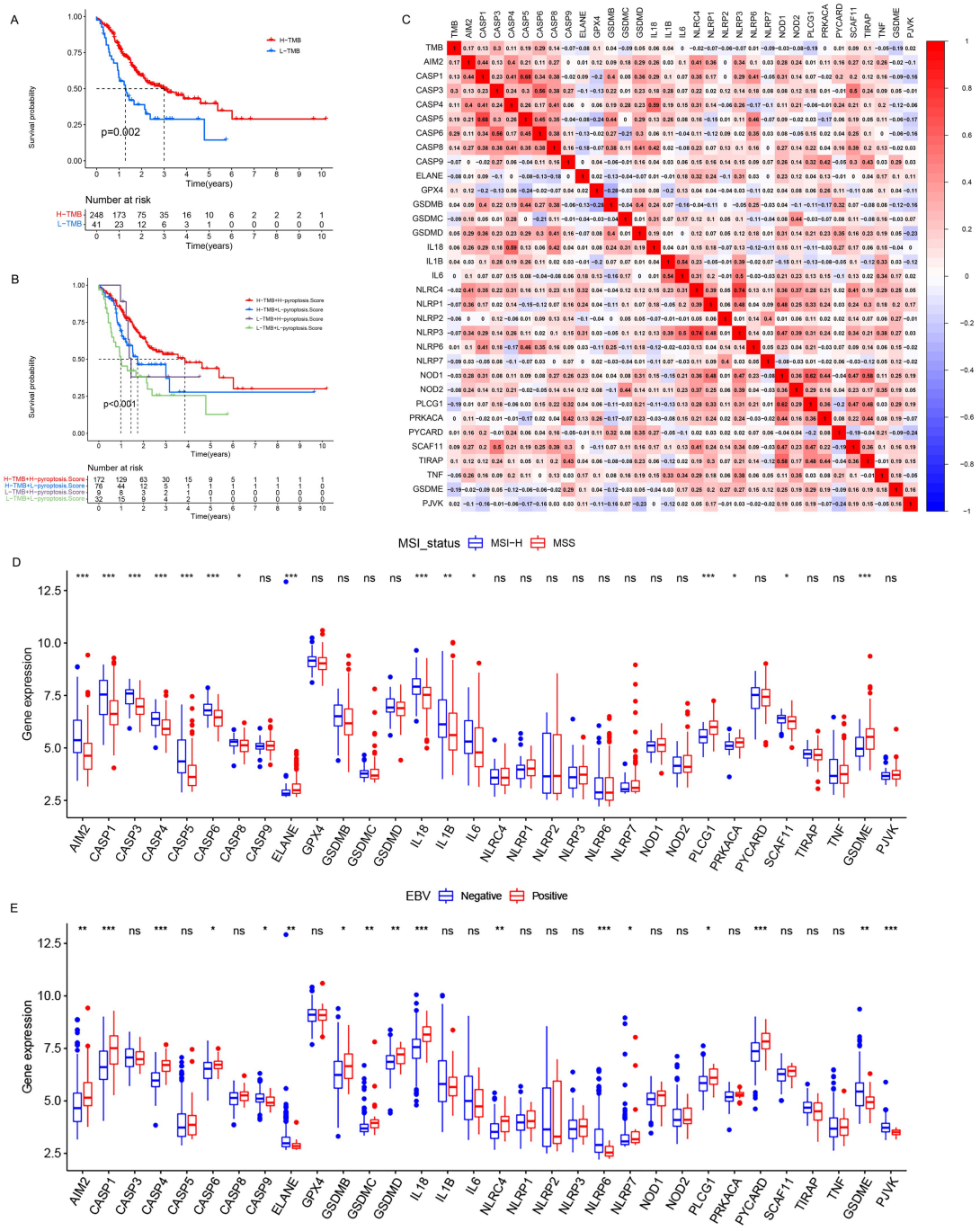

Figure S14. The effect of TMB, microsatellite status and EBV infection on PRs. (A) Survival analysis of TMB calculated based on the TCGA cohort (P = 0.002, Log-rank test). **(B)** Survival analysis for subgroup patients stratified by both TMB and PS using Kaplan-Meier curves. H, high; L, Low; (P < 0.001, Log-rank test). **(C)** Correlation analysis between TMB and PRs. **(D)** Difference in the expression of PRs between MSI and MSS subtypes. *P < 0.05; **P < 0.01; ***P < 0.001. **(E)** Difference in the expression of PRs between EBV-positive and EBV-negative groups. *P < 0.05; **P < 0.01; ***P < 0.001.

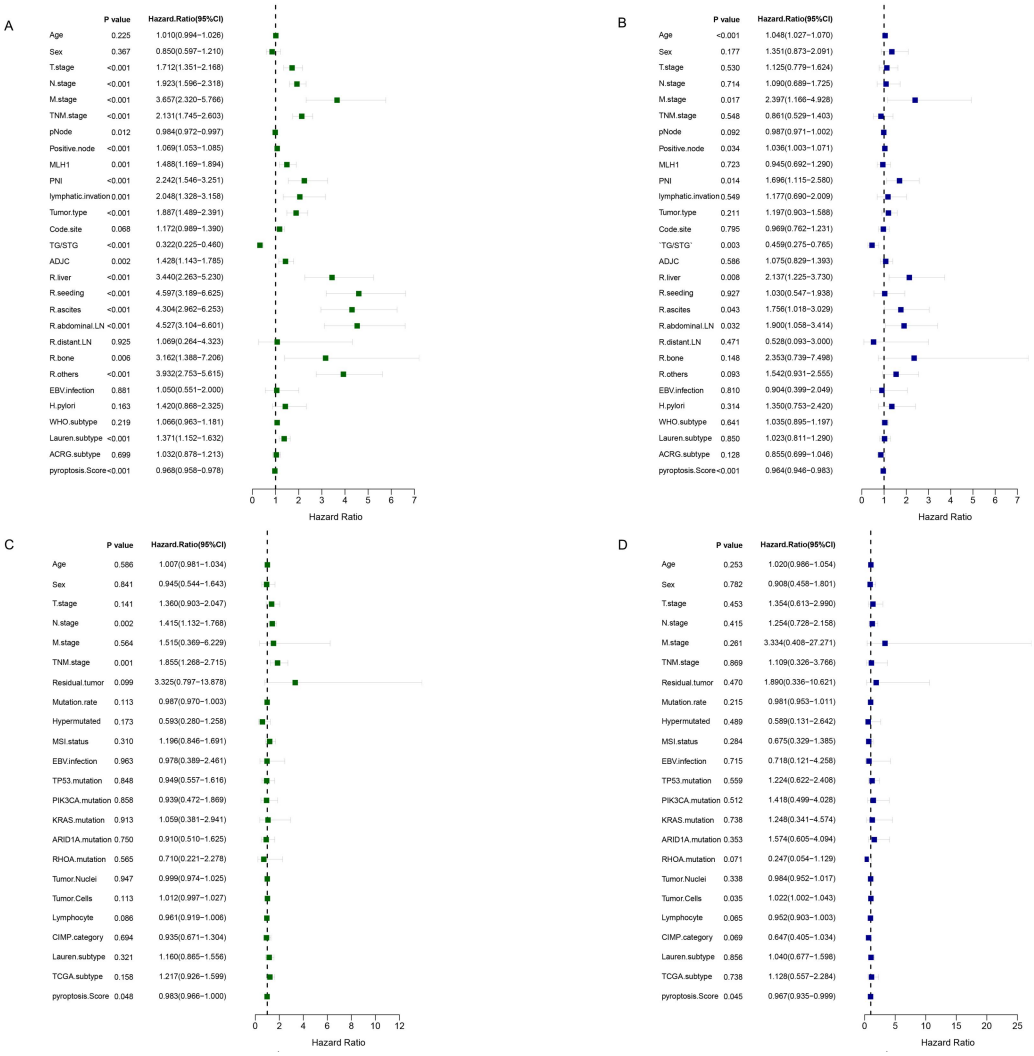

Figure S15. Independent prognostic analysis. (A) Univariate analysis for PS in GSE62254/ACRG cohort. **(B)** Multivariate analysis for PS in GSE62254/ACRG cohort. **(C)** Univariate analysis for PS in the TCGA cohort. **(D)** Multivariate analysis for PS in the TCGA cohort.

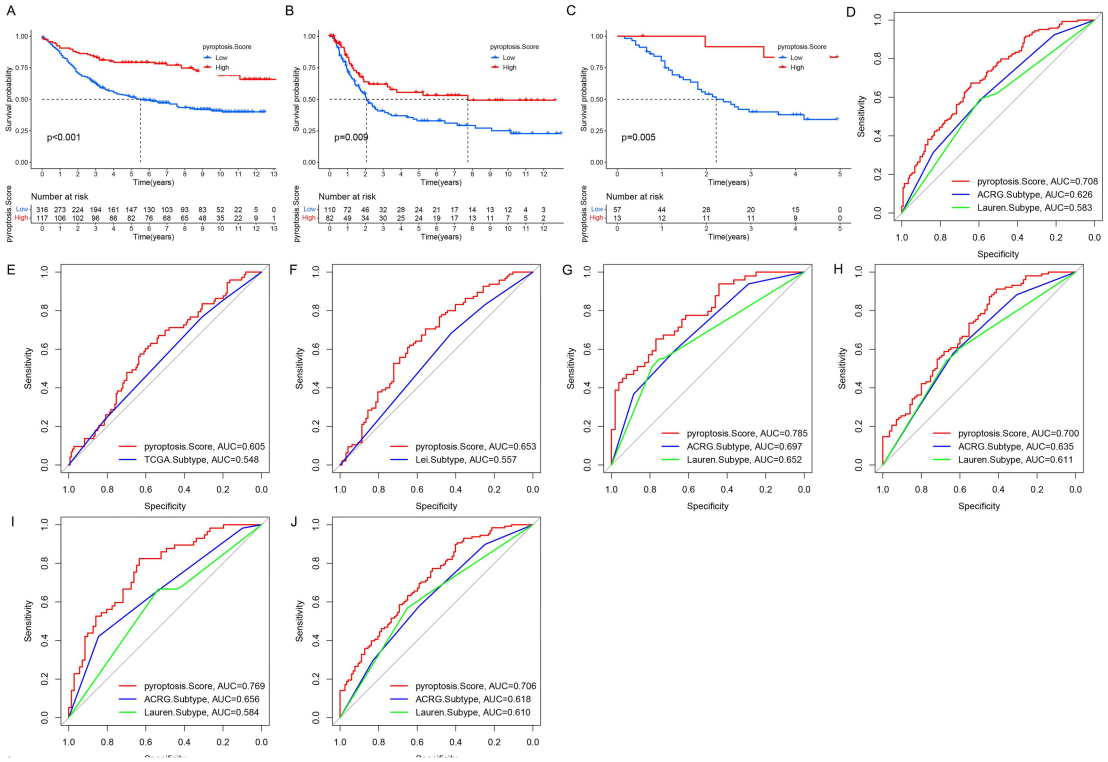

Figure S16. Prognostic value of PS in GC cohorts. (A) Survival analysis of PS in GSE84437 ($P < 0.001$, Log-rank test). **(B)** Survival analysis of PS in GSE15459 ($P = 0.009$, Log-rank test). **(C)** Survival analysis of PS in GSE57303 ($P = 0.005$, Log-rank test). **(D)** The predictive value of PS in GSE62254/ACRG cohort. **(E)** The predictive value of PS in the TCGA cohort. **(F)** The predictive value of PS in Lei cohort (GSE34942 and GSE15459). **(G)** The predictive value of PS in older patients (> 64) in GSE62254/ACRG cohort. **(H)** The predictive value of PS in young patients (< 64) in GSE62254/ACRG cohort. **(I)** The predictive value of PS in female patients in GSE62254/ACRG cohort. **(J)** The predictive value of PS in male patients in GSE62254/ACRG cohort.

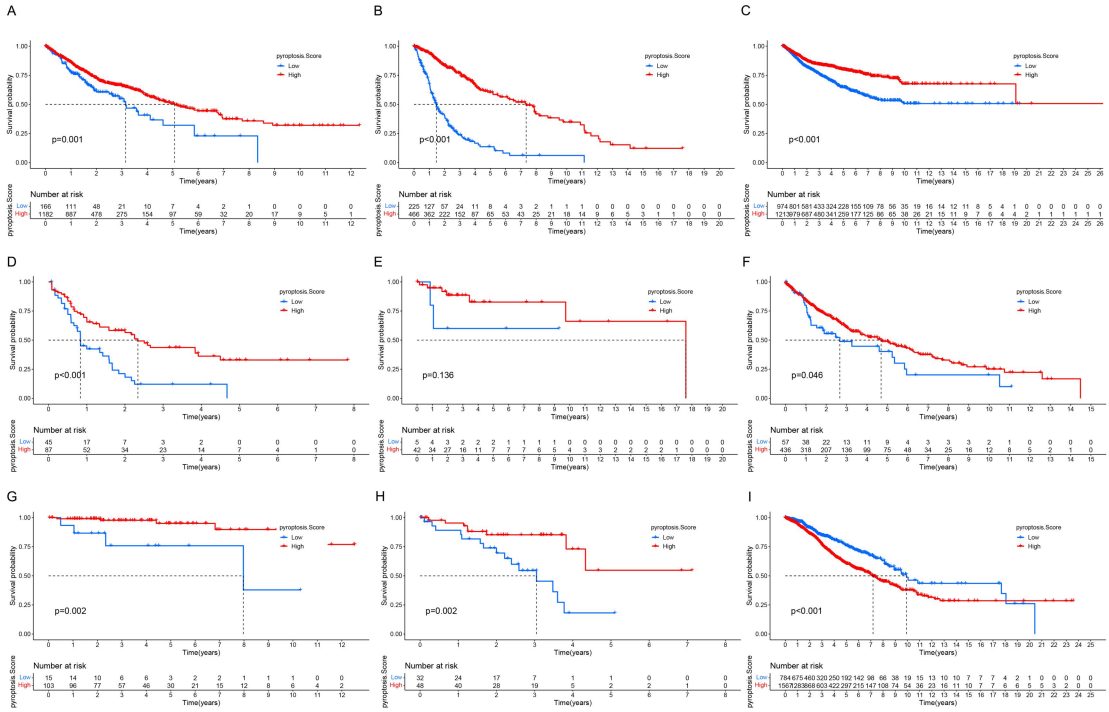

Figure S17. Prognostic value of PS in pan-cancer. (A) Survival analysis of PS in digestive system tumors including esophageal carcinoma, cholangiocarcinoma, liver hepatocellular carcinoma, pancreatic adenocarcinoma, colon adenocarcinoma and rectum adenocarcinoma (P = 0.001, Log-rank test). **(B)** Survival analysis of PS in nervous system tumors including glioblastoma multiforme and lower grade glioma (P < 0.001, Log-rank test). **(C)** Survival analysis of PS in urinary system tumors including adrenocortical carcinoma, bladder urothelial carcinoma, kidney chromophobe, kidney renal clear cell carcinoma, kidney renal papillary cell carcinoma, pheochromocytoma, paraganglioma, testicular germ cell tumor and prostate adenocarcinoma (P < 0.001, Log-rank test). **(D)** Survival analysis of PS in acute myeloid leukemia (P < 0.001, Log-rank test). **(E)** Survival analysis of PS in diffuse large B-cell lymphoma (P = 0.136, Log-rank test). **(F)** Survival analysis of PS in lung squamous cell carcinoma (P =0.046, Log-rank test). **(G)** Survival analysis of PS in thymoma (P = 0.002, Log-rank test). **(H)** Survival analysis of PS in uveal melanoma (P = 0.002, Log-rank test). **(I)** Survival analysis of PS in common tumors in women including breast invasive carcinoma, cervical squamous cell carcinoma, endocervical adenocarcinoma, uterine corpus endometrial carcinoma, uterine carcinosarcoma and ovarian serous cystadenocarcinoma (P < 0.001, Log-rank test).